Available online at www.sciencedirect.com
ScienceDirect
Optics Communications 267 (2006) 224–228
OPTICS COMMUNICATIONS
www.elsevier.com/locate/optcom

Raman scattering and fluorescence emission in a single nanoaperture: Optimizing the local intensity enhancement

Jérôme Wenger [a,*], José Dintinger [b], Nicolas Bonod [c], Evgeni Popov [a], Pierre-François Lenne [a], Thomas W. Ebbesen [b], Hervé Rigneault [a]

[a] Institut Fresnel, Université d'Aix-Marseille III, CNRS UMR 6133, Domaine Universitaire de Saint Jérôme, 13397 Marseille Cedex 20, France
[b] ISIS, Université Louis Pasteur, CNRS UMR 7006, 8 allée G. Monge, 67000 Strasbourg, France
[c] Commissariat à l'énergie atomique, Centre d'études scientifiques et techniques d'Aquitaine, BP2, 33114 Le Barp, France

Received 8 March 2006; received in revised form 31 May 2006; accepted 7 June 2006

Abstract

We investigate the potential of a single subwavelength aperture milled in an aluminium film to enhance the local electromagnetic field. We compare the Raman scattering of unadsorbed chlorobenzene molecules and the fluorescence emission of Cyanine-5 dyes, having the same excitation and collection setup for both experiments. For the optimal nanoaperture diameter, we report a clear enhancement factor of about 5 of the Raman scattering intensity per unit volume. Since Raman scattering probes the molecular vibrational levels and avoids the resonant pumping of a real excited state, the observed Raman enhancement is disconnected from the effects of the molecular energy levels alteration previously reported for fluorescent dyes. The observations are similar for both Raman and fluorescence experiments, and stand in good agreement with numerical electromagnetic computations of the excitation intensity inside the nanoaperture.

1. Introduction

Milling nanometric apertures in a metallic film is an intuitive way to manufacture new nanophotonics devices. Although this concept appears very simple, nanometric apertures bear attractive physical properties, arising mainly because an aperture milled in a real metal with finite thickness and conductivity is far different from the ideal case of a hole in an infinitely thin perfect conductor [1,2]. Among these properties, one can mention the ability to localize light in spots much smaller than the volume set by the diffraction theory [3], the excitation of local surface plasmon modes [4–6] or the edge effects due to current discontinuities [6,7].

A surprising phenomenon that also occurs around nanometric apertures is the enhancement of the fluorescence signal emitted inside the nanostructure. This effect was first investigated for fluorescent molecules dispatched over a periodic array of nanoapertures [8–11]. However, the relative influence of the local (single aperture) and collective (nanohole array) effects remains difficult to quantify for nanoapertures arrays. It is thus worth looking at the physical phenomena occurring at an isolated nanohole. Our team has recently devoted much attention to this point, showing that a single subwavelength nanowell could significantly enhance the fluorescence rate emitted by a single Rhodamine 6G molecule [12], with an enhancement factor up to 6.5 as compared to the emission rate per molecule in open solution.

To further investigate this optical enhancement effect in a single nanoaperture, we monitor the Raman scattering intensity of unadsorbed chlorobenzene molecules filling apertures of various diameters. This method directly probes the molecular vibrational levels, and avoids the resonant pumping of a real excited state, as for fluorescence. Thus, the observed Raman enhancement is disconnected

* Corresponding author. Tel.: +33 491288064; fax: +33 491288067.
E-mail addresses: jerome.wenger@fresnel.fr (J. Wenger), herve.rigneault@fresnel.fr (H. Rigneault).

0030-4018/$ - see front matter © 2006 Elsevier B.V. All rights reserved.
doi:10.1016/j.optcom.2006.06.032

from the effects of the molecular energy levels alteration found for fluorescent dyes in [12,13] (as indicated by a dramatic lifetime reduction).

In this paper, we report a clear enhancement factor of almost 5 of the Raman signal per unit volume, occurring for an aperture diameter close to the cut-off of the fundamental optical mode which may propagate inside the hole. To bridge the gap between fluorescence and Raman scattering inside an isolated nanohole, we also study the fluorescence emission of single Cyanine-5 molecules, using the same excitation and collection setup as for the Raman experiments. We show a marked increase of the fluorescence rate per molecule, which appears comparable to the Raman enhancement and stands in good agreement with numerical electromagnetic computations of the excitation intensity inside the aperture. Finally, we discuss the implication of these findings in the physical explanation of this phenomenon and give clues towards the optimal design of isolated nanowells for molecular analysis.

2. Experiment

Circular nanometric apertures of diameters ranging from 120 to 450 nm are milled thanks to focused ion beam technique in a 250 nm thick aluminium layer deposited on a microscope coverslip. To investigate the Raman and fluorescence emission of molecules inside one single nanohole, we developed a custom confocal Raman microspectrometer, which is also used to perform fluorescence correlation spectroscopy (FCS), see Fig. 1. For both the fluorescence and Raman scattering experiments, the excitation was provided by the same linearly polarized 633 nm HeNe laser (Melles Griot), tightly focused by a 40× microscope objective (Zeiss Apochromat) to illuminate one single nanohole. Without a nanoaperture, the observation volume is limited by the 50 μm confocal pinhole and was calibrated to 1.2 μm^3 thanks to FCS [14] performed on Cyanine-5 molecules in open solution.

For Raman scattering experiments, we directly used chlorobenzene as purchased from Sigma–Aldrich (concentration of 10 mol/L) and deposited a droplet over the sample. The chamber was then covered to avoid evaporation. The laser power was set to 1.5 mW at the microscope entrance to avoid damaging the sample. The Raman signal is collected by the same microscope objective, and is further separated from the excitation laser and elastically scattered light by a set formed by a dichroic mirror (Omega filters), holographic notch filter (Kaiser Optical) and long-pass filter (Omega filters). Thanks to these state-of-the-art optical filters, the laser line is efficiently filtered with an optical density greater than 9. The Raman signal was then directed towards a Jobin-Yvon 270 M spectrometer coupled with a liquid-nitrogen cooled CCD camera (SpectrumOne, Jobin-Yvon). The spectrometer was set to the following characteristics: 600 grooves per mm grating, 200 μm entrance slit, 900 s acquisition time for each nanoaperture (180 s for the reference spectrum of chlorobenzene in open solution). This setup provides a spectral resolution of about 20 cm^{-1}. To keep the laser focused on the nanoaperture during the whole acquisition, part of the reflected laser beam is measured by the avalanche photodiodes and used as an incoming signal for a servo-control of the nanopositioning piezo system.

The background noise originates mainly from the induced fluorescence at the aluminium/glass interface and from the detector dark noise. It is almost constant over the 500–1300 cm^{-1} spectral window investigated, with an average intensity of about 3000 total counts per pixel during the 900 s acquisition. For the analysis of the Raman spectra, a reference of the background noise was taken on the plane metal/glass interface (no aperture) with the same conditions as for the nanoaperture case. This noise level corresponds well with the background seen between the Raman peaks on the nanoaperture spectra. For further analysis, it was thus subtracted from the nanoaperture data.

To compare the Raman scattering results to the fluorescence emission inside one isolated nanoaperture, we used Cyanine-5 dyes (Invitrogen) in a phosphate-buffered saline solution (PBS buffer). These fluorescent molecules are

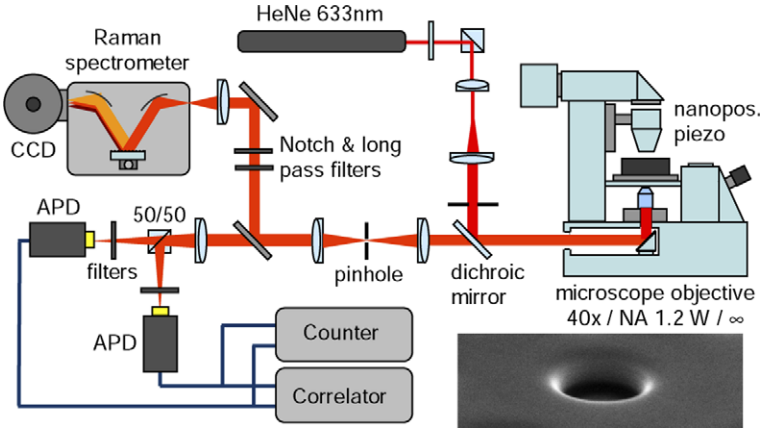

Fig. 1. Experimental setup for confocal Raman microspectroscopy and fluorescence correlation spectroscopy (APD: avalanche photodiode).

monitored thanks to FCS [12,15], which allows to determine both the average number of molecules in the observation volume and the detected average fluorescence count rate per molecule and per second. For fluorescence experiments, the laser power was carefully set to 15 μW to avoid saturation and photobleaching of the dye.

3. Raman enhancement estimation

Fig. 2 displays typical Raman spectra acquired for single nanoapertures filled with chlorobenzene in liquid solution, together with a reference confocal spectrum of the chlorobenzene solution. The well-known Raman peaks of chlorobenzene at 700, 1000 and 1080 cm^{-1} clearly emerge from experimental fluctuations (the two peaks around 830 and 900 cm^{-1} come from the backscattering of the HeNe laser plasma). Since the nanoapertures are filled with permanently diffusing chlorobenzene molecules and since the aluminium film is naturally protected by an oxide layer, we assume that the effect of molecule adsorption on the metal surface remains negligible. Due to the low efficiency of the Raman process (as compared to fluorescence), the acquisition time has to be extended up to 15 min for each nanoaperture spectrum, the CW laser power being kept at 1.5 mW to avoid any damage of the sample.

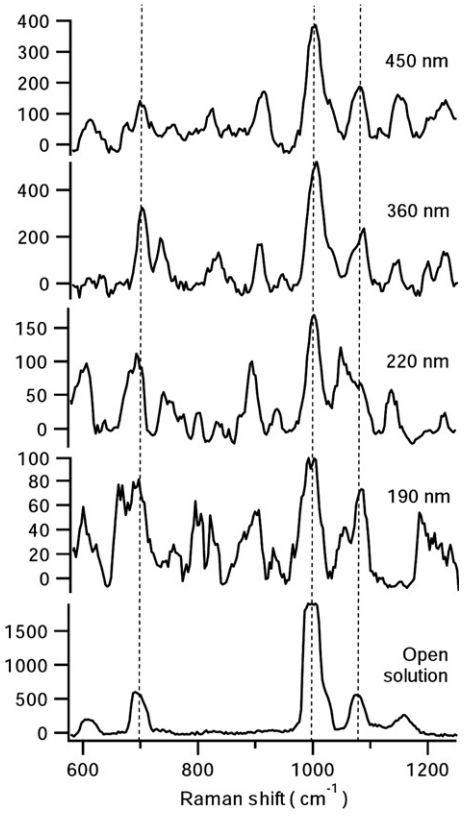

Fig. 2. Typical confocal Raman spectra (noise subtracted) obtained for 450, 360, 220 and 190 nm diameter nanoapertures filled with a pure chlorobenzene solution (900 s acquisition), together with the reference Raman spectra for the same open solution (180 s acquisition), with an excitation power of 1.5 mW at 633 nm. The vertical units correspond to the total number of counts per CCD pixel during the whole acquisition.

To investigate the potential of each nanoaperture to enhance the Raman signal, we introduce the Raman enhancement factor η_R as the ratio between the integrated intensity of a Raman peak per second and per unit volume inside the nanoaperture and in the open solution:

$$\eta_R = \frac{(I_{R,aper}/V_{aper})}{(I_{R,sol}/V_{sol})}, \quad (1)$$

where $I_{R,aper}$ and $I_{R,sol}$ are the integrated Raman intensity per second in a specific Raman band taken for the nanoaperture and the open solution respectively, V_{aper} and V_{sol} are the (confocal) effective observation volume for the nanoaperture and the open solution experiments respectively. $I_{R,aper}$ and $I_{R,sol}$ are readily obtained from the experimental spectra displayed in Fig. 2. In open solution, the confocal volume V_{sol} is calibrated to 1.2 fL from fluorescence correlation spectroscopy performed on Cyanine-5 molecules. Inside the nanohole, V_{aper} is numerically computed following [16] using a rigorous resolution of Maxwell's equations for the excitation field E in cylindrical coordinates [17]:

$$V_{aper} = \frac{\left(\int_V |E|^2 dV\right)^2}{\int_V |E|^4 dV}, \quad (2)$$

where the integration is performed over the entire nanoaperture volume. This volume appears close to the aperture geometrical volume, as probed by FCS experiments [12], and shown by the inset in Fig. 3. As a supplementary check that all the detected signal came from the nanoaperture and not from the solution above, we used fluorescent spheres of 2 μm diameter (Molecular Probes) fixed over the nanoaperture to measure the epi-detected fluorescence. From the detected light level, a maximum height of 80 nm of the solution directly above the nanoaperture can be inferred to contribute to the epi-detected signal in the case of the largest aperture diameter. This height then rapidly decreases as the aperture diameter becomes smaller. The uncertainty on the determination of the effective probed volume V_{aper} within the aperture leads at most to a 30% overestimation on η_R, which falls into the errors bars range in Fig. 3.

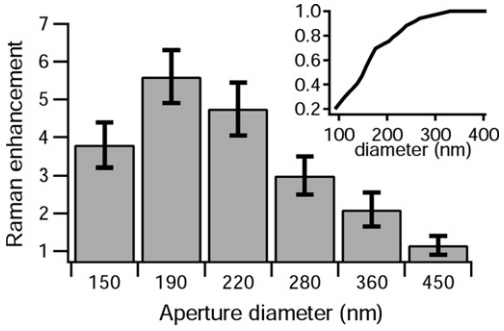

Fig. 3. Raman enhancement factor η_R versus the nanoaperture diameter, as defined by Eq. (1). The inset shows the ratio of the effective excitation volume V_{aper} numerically computed from Eq. (2) to the aperture geometrical volume versus the aperture diameter.

To give an estimate of the enhancement factor η_R, we take into account three major Raman bands displayed in Fig. 2: 674–720, 968–1037 and 1053–1098 cm^{-1}. The average enhancement factor obtained for these three bands is then computed according to Eqs. (1) and (2), which yields the results displayed in Fig. 3. A significant Raman enhancement of about 5 is observed for aperture diameters around 190 nm, which is close to the cut-off of the fundamental mode which can propagate through the aperture. Obviously, these results are still far away from the Raman enhancement reported for SERS experiments on colloidal clusters [18]. However, the present study helps the understanding of the physical phenomena occurring at a single nanoaperture (see discussion below). Let us also stress that we presently do not investigate surface enhancement effects such as in SERS, but rather concentrate on the Raman emission from the bulk liquid solution of calibrated volume.

4. Comparison with fluorescence enhancement and theoretical computations

It is informative to compare the Raman enhancement η_R with the fluorescence enhancement η_F, defined as the ratio between the detected count rate per molecule inside the aperture and the detected count rate per molecule in open solution. η_F is measured from fluorescence correlation spectroscopy experiments in a nanohole and in open solution to evaluate the respective detected count rates per molecule. These count rates are obtained by dividing the total average photocounts per second by the average number of detected molecules N, which is computed from the autocorrelation value at the origin [12]. Let us mention that this procedure is independent of the shape of the excitation field and the type of the diffusion statistics:

$$g^{(2)}(0) = 1 + \frac{1 + n_{off}}{N}\left(1 - \frac{\langle b\rangle}{\langle i\rangle}\right)^2. \quad (3)$$

n_{off} stands for the dark-state amplitude, $\langle i\rangle$ is the mean intensity and $\langle b\rangle$ the mean background. For each experimental run, the dark-state amplitude n_{off} was fitted to the autocorrelation function, and the fraction of molecules in the non-emitting state defined as $n_{off}/(1 + n_{off})$ was found in the range of about 45% for the various aperture sizes. This corresponds well to the photostationary equilibrium established between the Cyanine-5 isomeric forms reported in [19]. The excitation power was set to 15 μW to avoid fluorescence saturation and photobleaching. We checked that the average number of molecules and the mean diffusion time remained constant while increasing the excitation power up to 50 μW in open solution as well as in the nanoaperture.

The detected fluorescence rate per molecule needed to compute η_F is then readily obtained by dividing the total average number of photocounts per second by the average number of molecules N. Fig. 4 shows a typical fluorescence intensity autocorrelation function obtained for Cyanine-5 molecules diffusing across a 190 nm aperture and the corresponding numerical fit assuming a 3D Brownian diffusion.

Fig. 5 displays the fluorescence enhancement η_F for several aperture diameters. As for the Raman enhancement η_R, we obtain a clear peak for a 190 nm aperture, with a maximum enhancement of 7.0. This curve appears fully consistent with the observations reported for Rhodamine 6G in aqueous solution inside the nanoapertures [12], where a maximum enhancement of 6.5 was reported for a 150 nm aperture. The difference between the optimal aperture diameter for both dyes can be directly understood as a scale change arising from the different excitation wavelength used, as the wavelength to diameter ratio remains almost the same for 488 and 633 nm excitations ($633/190 \approx 3.33$, while $488/150 \approx 3.25$).

Finally, using a rigorous electromagnetic theory of light propagation in a single nanoaperture, we computed the electric field intensity per unit of effective volume η_{ex} as a function of the aperture radius for the excitation field [20], defined as

$$\eta_{ex} = \frac{\int_V |E|^2 dV}{V_{aper}}, \quad (4)$$

where the integration is performed over the entire nanoaperture volume, taking chlorobenzene as the filling medium

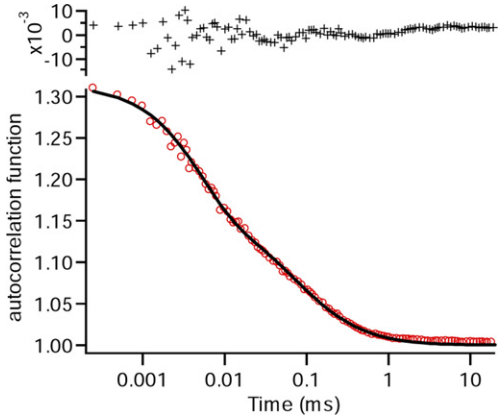

Fig. 4. Fluorescence autocorrelation function obtained for Cyanine-5 molecules diffusing across a 190 nm aperture (circles) and numerical fit (line) assuming a 3D Brownian diffusion. The upper graph shows the residuals of the fit.

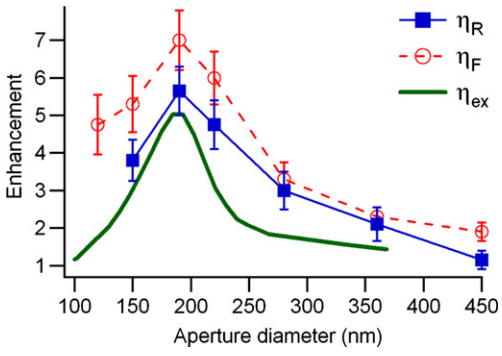

Fig. 5. Raman enhancement η_R (squares, solid line), fluorescence enhancement η_F (circles, dashed line) and excitation intensity enhancement η_{ex} (thick line) versus the nanoaperture diameter.

(refractive index of 1.52). The variation of η_{ex} versus the aperture diameter is displayed in Fig. 5 and follows well the experimental Raman enhancement η_R.

5. Discussion

Altogether, the results reported in Fig. 5 support the idea that almost all the optical emission enhancement observed in nanoholes can be understood as an increase of the excitation intensity within the aperture. The case of Raman scattering is particularly informative because it is disconnected from the alteration of the molecular energy levels branching ratios found previously for fluorescent dyes.

The increased signal could also originate from a higher collection efficiency for an emitter located inside a nanoaperture. However, since the high aperture microscope objective already collects 30% of the emitted light in open solution, we expect the increase in η_R and η_F to be at most a factor of 3.3, which is clearly not enough to account for the experimental observations. Nevertheless, the influence of the aperture on the local collection efficiency may play a role in the discrepancy between the experimental data and the theoretical model. This effect still needs to be taken into account to completely model the experiments.

Another way of considering the optical enhancement inside a single nanohole is to have a look at the total detected signal versus the effective volume being probed. Investigating linear processes such as fluorescence or Raman scattering, one would naively expect the detected signal in a nanoaperture to decrease linearly with the observation volume. However, dealing with properly chosen nanoapertures, the signal decrease due to the smaller volume can be somehow offset by the reported optical enhancement. This is illustrated in Fig. 6 which shows the detected signal (awaited) versus the volume reduction (normalized such that a volume of one provides a signal of one). Thanks to the optical enhancement in a subwavelength aperture, the detected total signal arising from an aperture at the optimal diameter can be quite as high as

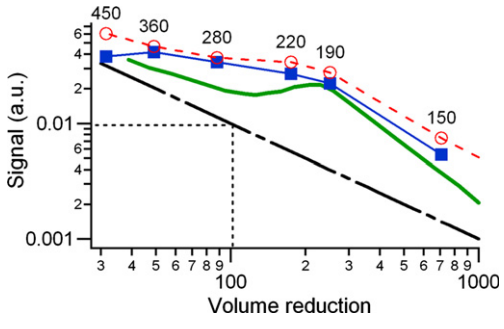

Fig. 6. Total detected signal per nanoaperture versus the volume reduction as compared to a standard confocal experiment (the vertical scale is normalized such that a volume of one provides a signal of one). Dash-dotted line: naïve linear dependence (slope of 1), Thick line: signal awaited from the excitation intensity enhancement η_{ex}, squares: Raman signal from η_R, circles: fluorescence signal from η_F. The figures above the markers indicate the corresponding aperture diameter in nm.

the signal collected from a 5–7 times larger aperture, overcoming the signal reduction from the smaller volume. This surprising phenomenon brings new insights towards the optimal design of nanowells for chemical analysis.

6. Conclusion

Nanometric apertures in a metallic film are easy to produce, robust and highly reproducible nanophotonic devices to probe chemical reactions in volumes below the diffraction limit. In this paper, we provide a clear experimental evidence of Raman scattering enhancement in a nanoaperture filled with a liquid solution of Raman-active molecules. Our results still lie far away from the enhancement factors reported in SERS experiments [18,21], nevertheless this work contributes to the understanding of the physical phenomena occurring at a single nanostructure, and opens the way towards surface-enhanced Raman scattering in a single nanoaperture. This would provide a reproducible and easy-to-produce substrate for enhanced Raman analysis, originating either from spontaneous scattering or stimulated coherent anti-Stokes Raman scattering (CARS).

References

[1] H.A. Bethe, Phys. Rev. 66 (1944) 163.
[2] T.W. Ebbesen, H.J. Lezec, H.F. Ghaemi, T. Thio, P.A. Wolff, Nature 391 (1998) 667.
[3] E.H. Synge, Philos. Mag. 6 (1928) 356.
[4] H.J. Lezec, A. Degiron, E. Devaux, R.A. Linke, L. Martin-Moreno, F.J. Garcia-Vidal, T.W. Ebbesen, Science 297 (2002) 820.
[5] A. Degiron, H.J. Lezec, N. Yamamoto, T.W. Ebbesen, Opt. Commun. 239 (2004) 61.
[6] E. Popov, N. Bonod, M. Nevière, H. Rigneault, P.F. Lenne, P. Chaumet, Appl. Opt. 12 (2005) 2332.
[7] R. Zakharian, M. Mansuripur, J.V. Moloney, Opt. Express 12 (2004) 2631.
[8] Y. Liu, S. Blair, Opt. Lett. 28 (2004) 507.
[9] Y. Liu, J. Bishop, L. Williams, S. Blair, J. Herron, Nanotechnology 15 (2004) 1368.
[10] Y. Liu, F. Mahdavi, S. Blair, IEEE J. Sel. Top. Quant. Electron 11 (2005) 778.
[11] A.G. Brolo, S.C. Kwok, M.G. Moffitt, R. Gordon, J. Riordon, K.L. Kavanagh, J. Am. Chem. Soc. 127 (2005) 14936.
[12] H. Rigneault, J. Capoulade, J. Dintinger, J. Wenger, N. Bonod, E. Popov, T.W. Ebbesen, P.F. Lenne, Phys. Rev. Lett. 95 (2005) 117401.
[13] J. Wenger, P.F. Lenne, E. Popov, H. Rigneault, J. Dintinger, T.W. Ebbesen, Opt. Express 13 (2005) 7035.
[14] D. Magde, E. Elson, W.W. Webb, Phys. Rev. Lett. 29 (1972) 705.
[15] M.J. Levene, J. Korlach, S.W. Turner, M. Foquet, H.G. Craighead, W.W. Webb, Science 299 (2003) 682.
[16] R. Rigler, U. Mets, J. Windengren, P. Kask, Eur. Biophys. J. 22 (1993) 169.
[17] N. Bonod, E. Popov, M. Nevière, J. Opt. Soc. Am. A 22 (2005) 481.
[18] K. Kneipp, H. Kneipp, I. Itzkan, R.R. Dasari, M.S. Feld, Chem. Rev. 99 (1999) 2957.
[19] J. Widengren, P. Schwille, J. Phys. Chem. A 104 (2000) 6416.
[20] E. Popov, M. Nevière, J. Wenger, P.F. Lenne, H. Rigneault, P.C. Chaumet, N. Bonod, J. Dintinger, T.W. Ebbesen, Anomalous field enhancement in single subwavelength apertures, J. Opt. Soc. Am. A, Available online: 16 March 2006.
[21] A.G. Brolo, E. Arctander, R. Gordon, B. Leathem, K.L. Kavanagh, Nano Lett. 4 (2004) 2015.